

Reinforced Concrete Shear Walls with De-bonded Diagonal Reinforcements for the Damage-less Reinforced Concrete Building

Kazushi Shimazaki

Professor, Dept. of Architecture and Building Engineering, Kanagawa University, JAPAN
Email: shimazaki@kanagawa-u.ac.jp

ABSTRACT :

Recently, owners of buildings wish to continue using their buildings with low repair cost even after a severe earthquake. To achieve this, it is necessary to reduce the damage or to ensure good repairability of members. For a reinforced concrete building with a “shear core”, as the core resists most of the seismic force, large shear force and bending moment occurs. Repairability of the core wall is one of the most important factors in order to reuse the building. This paper examines the behavior of shear walls with de-bonded diagonal reinforcements to reduce the damage and so ensure good repairability.

Test results showed that the number of cracks differed greatly even for the same load-carrying capacity; the total length of diagonal shear cracks was significantly less for walls with de-bonded diagonal reinforcements. Repair work was easier than with the common parallel reinforced wall. For precast walls, horizontal cracks appeared only at the bottom end of the wall; no diagonal cracks were observed, and these walls were easy to repair. For all specimens except the walls having an orthogonal wall, the maximum load was kept until $R = 1/67$. For the walls having an orthogonal wall, the load degraded during cyclic loading at $R = 1/100$ caused by compressive failure of concrete to resist the large amount of tension reinforcements in the orthogonal wall. It is difficult to reuse these walls after large deformation. The load-deflection relationship for all the specimens with diagonal reinforcements showed the slip property after $R = 1/100$. The equivalent viscous damping factor was smaller than the value of the wall with parallel bars.

In conclusion, the newly developed earthquake resisting wall reduces damage, shows good performance, and can be reused even after a severe earthquake.

KEYWORDS: reinforced concrete structure, damage control, shear wall, earthquake resistant design, diagonal reinforcement, bond

1. INTRODUCTION

The goal of earthquake resistant design in any country is to protect life in very severe earthquakes by providing buildings with the strength and durability required to resist collapse. After a severe earthquake such as the Great Hanshin Earthquake, however, the demands of building owners changed: they want to be able to use the buildings again, at a low repair cost. In response, damage control design has recently become popular. This requires good repairability even for RC members to improve the performance of the member. On the other hand, the performance requirements of buildings during planning are diverse, such as improved habitability and large open spaces for flexibility. The hybrid structural system combined with RC core walls connected by damper beams, CFT columns, and flat plate slabs as shown in Figure 1 is one structural type which meets these performance requirements. In this structural system, a large part of the horizontal force is resisted by the core wall, and most of the energy of the earthquake is absorbed in parts such as the boundary beam damper connected to the core walls. The CFT columns are mainly provided for supporting the vertical force. It has been reported that it was possible to reduce the damage of the boundary beam by using de-bonded diagonal reinforcement bars [shimazaki, 2004]. The performance of CFT column-flat plate joints has also been reported [Sato & shimazaki, 2004].

On the other hand, as a large part of the horizontal force is to be resisted in the core walls, severe shear force and bending moment act at the bottom of the walls. Diagonal cracks caused by this shear force reduce the shear stiffness of the core wall substantially. As shear stiffness cannot be restored by repair works, it is desirable to

minimize such diagonal cracks. The horizontal cracks caused by bending moment will be closed by the action of the dead load after an earthquake; this damage, unless severe, is acceptable.

To improve the performance of the earthquake resistant wall, a 45-degree arrangement of bars, the combination of precast and pre-stressed, and removal of the bond of the main reinforcement of the wall and so on have been proposed[Sittipunt et al. 2000, Yahya et al. 2002, FIB 2003]. The objectives of these proposals were to ensure good ductile capacity, not to reduce the damage. In order to reduce the damage and to make a precast member for the core wall of the prototype building shown in Figure 1, this study tested the damage reduction type earthquake resistant wall having de-bonded X type reinforcing bars which are expected to act as a brace.

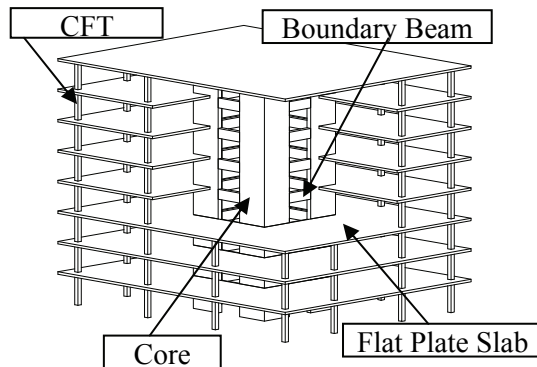


Figure 1 Prototype Building

2. Experiment

2.1. Specimens

Six wall specimens of 1800-mm height, 900-mm width and 120-mm thickness were tested. They were part of the lower 2.5 stories of the prototype building shown in Figure 1. Following a preliminary analysis, the top of the specimen is at the height of the point of contraflexure of the first story core wall. The section arrangements of bars are shown in Table 1 and Figure 2.

Table 1 Test specimens

Specimen		WP1	WX1	WSX1	WSX2	WTX1	WTX2
b×D(mm)	Main Panel			120×900			
	Orthogonal					350×120	
σ_b (N/mm ²)		44		43		43	
Vertical bars	End	6-D13 ($\sigma_y=371$ N/mm ²)	6-D6 ($\sigma_y=368$ N/mm ²)	12-D13 ($\sigma_y=390$ N/mm ²)		14-D13 ($\sigma_y=368$ N/mm ²)	
	Center	14-D13 ($\sigma_y=371$ N/mm ²)		14-D13 ($\sigma_y=368$ N/mm ²)		6-D6 ($\sigma_y=374$ N/mm ²)	4-D6、2-D16
	Orthogonal					8-D16 ($\sigma_y=388$ N/mm ²)、6-D6	
Diagonal bars		12-D13 ($\sigma_y=371$ N/mm ²)		12-D13 ($\sigma_y=376$ N/mm ²)		12-D13 ($\sigma_y=376$ N/mm ²)	
Horizontal bars		2-D10@70 ($\sigma_y=387$ N/mm ²)		2-D10@70 ($\sigma_y=353$ N/mm ²)		2-D10@70 ($\sigma_y=353$ N/mm ²)	
Confining bars	Upper	2-D6@70 ($\sigma_y=368$ N/mm ²)		2-D6@70 ($\sigma_y=374$ N/mm ²)		2-D6@70 ($\sigma_y=374$ N/mm ²)	
	Lower					2-D6@35 ($\sigma_y=374$ N/mm ²)	

WP1 is a common parallel reinforced wall. WX1 has de-bonded diagonal reinforcements arranged instead of the edge vertical reinforcing bars of 6-D13 of WP1, and additional 6-D6 were arranged at that place for confining bars. To de-bond the reinforcing bars, de-bond tape (butyl type rubber, Saint Tuck Sheeler) and gummed tape were used.

WSX1 was divided at each story assuming a precast panel, and WSX2 has crack generation plates of 0.6-mm

thickness which divide the panel horizontally into three parts. Each gap between the panels was filled with grout mortar. The edge vertical reinforcement of both WSX1 and WSX2 was de-bonded and fixed at the panel boundary by fixing plates of 40x40x6 mm and nuts as shown in Photograph 1. The other reinforcements in the panel were the closed type and were anchored in it.

WTX1 is a T-shape specimen with an orthogonal wall for concentration of the L type flange wall. WTX2 has D16 reinforcing bars instead of D6 at the other end of the flange wall (hereafter called “free end”). The bar is cut off at 160 mm in the lower stub, and de-bonded in the stub. This is expected to increase the compressive strength at the free end and not increase the tensile strength. The former prevents concrete crushing caused by the large tensile strength of the orthogonal wall, and the latter prevents an increase in the number of cracks.

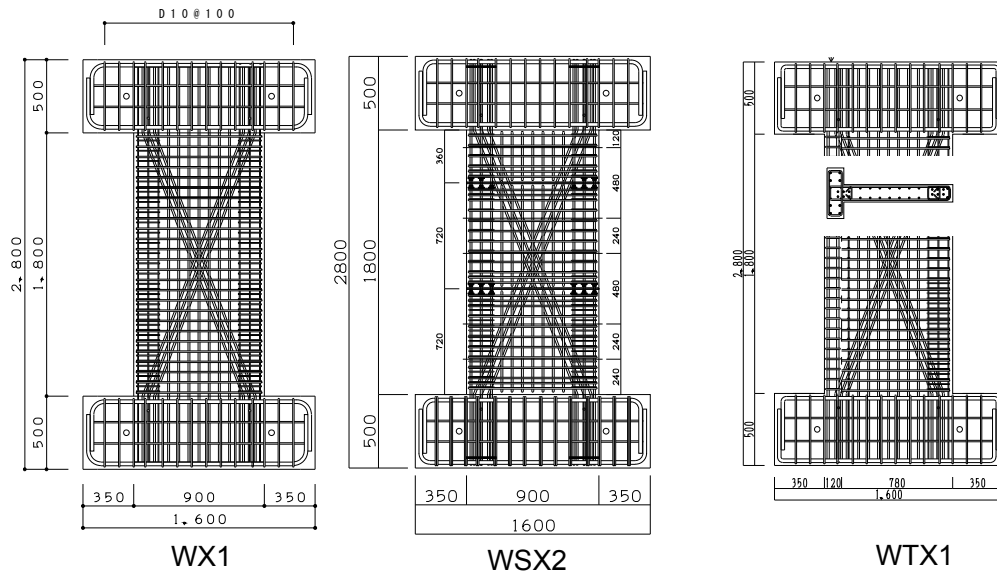


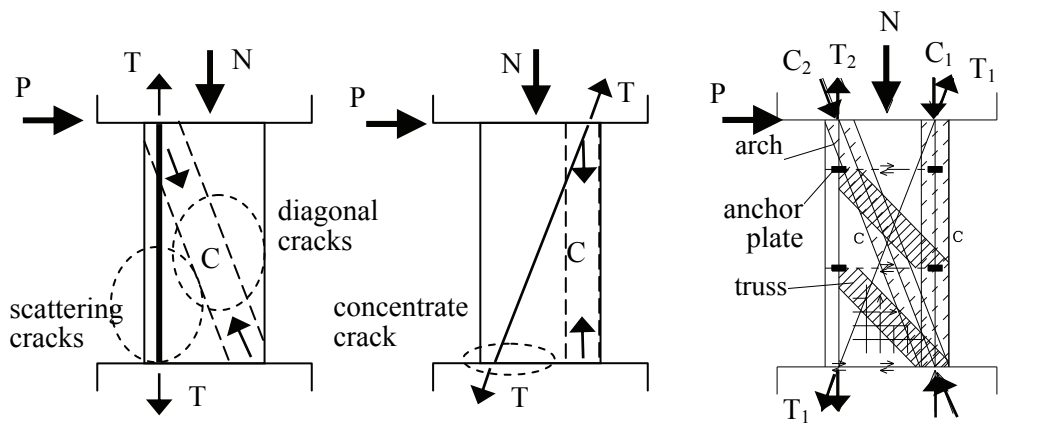
Figure 2 Section arrangements of bar for typical specimens



Photo 1 Fixing plates of de-bonded vertical rebar

2.2. Model of load-resistant mechanism

The assumed model of the load-resistant mechanism is shown in Figure 3. For the common type wall, when the horizontal force acts from the left side as shown in Figure 3a), as the tension force occurs in the left side, many bending cracks are generated. In the center of the panel, a diagonal crack occurs due to shear force. For the de-bonded diagonal reinforced wall, the tension force is mainly resisted by X type reinforcing bars (T) as shown in Figure 3b), and at the edge part of the wall on the left side, the tension force is very small due to only the thin vertical reinforcing bars arranged as confining bars. Therefore, the cracks are expected to be concentrated only at the bottom of the panel, and the total number and length of cracks are decreased substantially. For WSX, the divided panel wall type, the horizontal force is resisted by the edge vertical reinforcement, the tension of the X type main reinforcement, and the compression force of concrete as shown in Figure 3c). The total number of horizontal cracks is expected to decrease by concentrating them at the division part, hence the bending deformation is dominant and the diagonal cracks are reduced. The de-bonded edge vertical reinforcements have anchor plates at the division part and a truss mechanism is formed in every panel as shown in Figure 3c).



a) common type wall b) de-bonded diagonal reinforced wall c) divided panel wall

Figure 3 Load-resistant mechanism model

2.3. Loading and measurement

Cyclic horizontal force is applied at the top of the wall under constant axial compression load of 392 kN for the plane type walls, and 490 kN for the T shape walls. The loading cycle is one cycle at $R = 1/700$, three at $R = 1/400$ and $1/200$, six at $R = 1/100$, three at $R = 1/67$, and finally one way loading to $R = 1/33$.

Total horizontal displacements at the top and each story and partial vertical displacements to calculate the curvature for bending deformation are measured. Also, strain gauges are attached to the main reinforcing bars.

3. Experimental results

3.1. Crack pattern

Crack patterns at $R = 1/200$ and $1/100$ of each test specimen are shown in Figure 5. Bending cracks occurred in the cycle at $R = 1/700$ for all test specimens. Bending shear cracks occurred at $R = 1/400$ for WP1, WTX1 and WTX2, and at $R = 1/200$ for WX1.

At $R = 1/200$, the diagonal bending shear crack was conspicuous for WP1, whereas for WX1, the horizontal crack region was wide and there were few diagonal shear cracks. For WTX1 and WTX2, when the orthogonal wall side became compressed, horizontal cracks were observed in the tension side but when the orthogonal wall side became tension, only diagonal cracks were observed. Also, few diagonal cracks were observed in WSX1 and WSX2.

At $R = 1/100$, signs of concrete crushing in the bottom part were observed for WP1, WX1, WSX1 and WSX2. The crack width except at the bottom boundary at $R = 1/100$ was 0.2 mm for WP1, and 0.05 mm for WX1. For WTX1, the edge D6 reinforcing bars buckled and fractured during repeating loading at $R = 1/100$. The concrete crushed region expanded to the central part with increasing damage to the edge. For WTX2 at $R = 1/100$, concrete crushing stayed in the concrete surface. For WSX1 and WSX2, the diagonal cracks decreased substantially compared with WX1. The remaining crack width at the bottom boundary of the wall panel was about 0.4 mm for both WSX1 and WSX2.

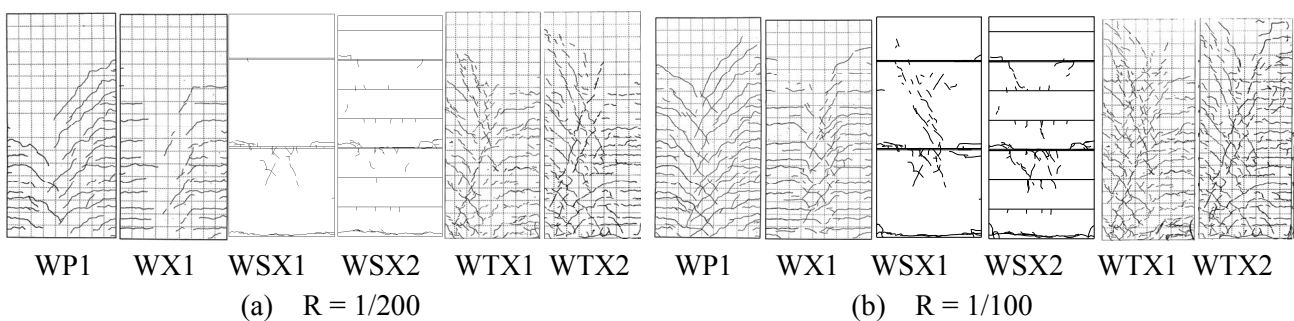


Figure 5 Crack pattern

At $R = 1/67$, for WTX1, the concrete crushing progressed in both end parts, and for WTX2, it progressed into the center part.

At $R = 1/33$, the concrete crushed part progressed in both end parts for WP1, WX1, WSX1 and WSX2, however the axial load was maintained until the last cycle. Hence, the deformation capacity is sufficient.

3.2. Load-deflection curves

The relationships of horizontal force and top displacement of the specimens are shown in Figure 6. For all specimens except the T-shape model, the maximum load was maintained until at $R = 1/67$, after which the strength declined gradually. For WX1, the vertical reinforcement of D6 in the edge part buckled at $R = 1/40$ and the strength declined. For WTX1, after the strength declined at $R = 1/100$, concrete was crushed in the compression side, and D6 reinforcements broke. Then, in the test the cycle was reduced once at $R = 1/67$, and additional one-way loading for the orthogonal wall compression side was performed until $R = 1/40$. For WTX2, the control displacement of the first cycle at $R = 1/67$ exceeded the target value caused by range-over of the control displacement gauge and the data could not be obtained. The gray line in the figure is the value estimated from the test minute. At $R = 1/100$ cycle, even concrete was crushed in the unconfined region, the strength kept the maximum value, and the strength declined at $R = 1/67$ caused by buckling of D13 rebars. In the figure, the solid and dashed lines are calculated values as described in Section 4.1.

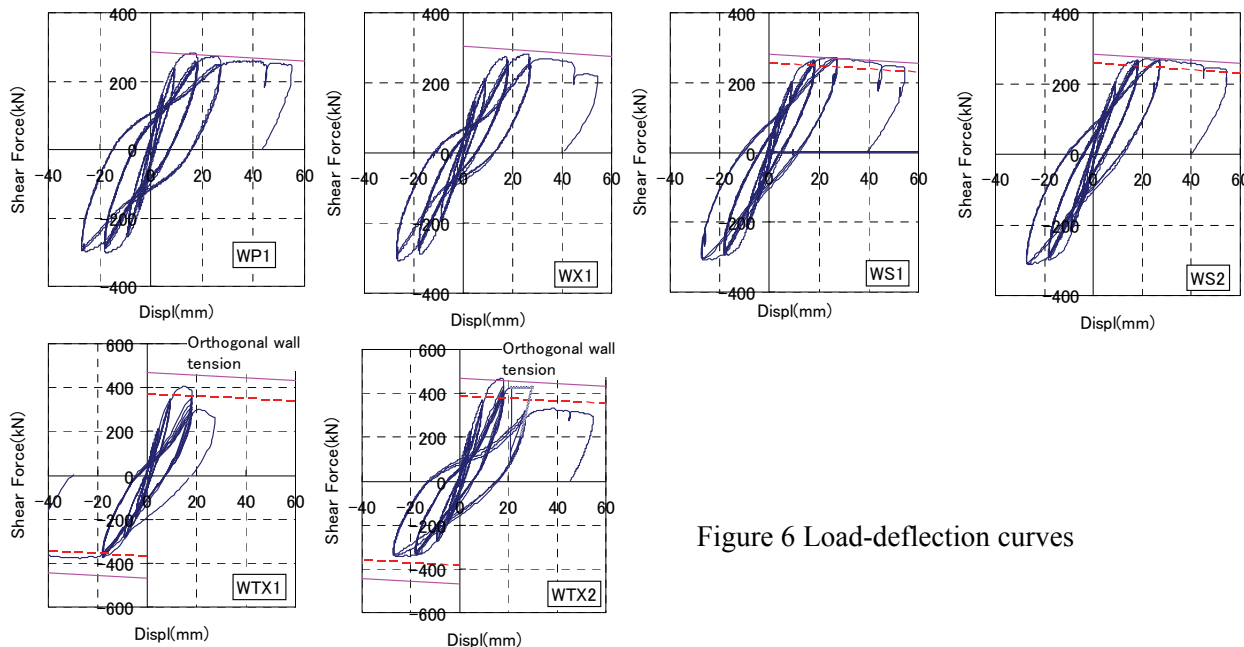


Figure 6 Load-deflection curves

3.3. Strain of reinforcements

Figure 7 shows the strain distribution of the typical main reinforcements. The vertical reinforcement of both edges of WP1 was as shown in Figure 7a); both tension-compression bars yielded, and the stress fully reached the yield stress. The de-bonded X type compression bar of WX1 shown in Figure 7b) became about 1/4 of the yield strain. For WSX1 and WSX2, the strain of X reinforcements in the compression side became about 1/2 compared with the tension side as shown in Figure 7c)d). The vertical reinforcement of both edges yields at the first story in WSX1, and stays in the yield strain for WSX2 which is confined in the compression region. For WTX1 and WTX2 which have the orthogonal wall, the strain of the X reinforcements is about 2/3 of the yield strain of both compression and tension steel when the orthogonal wall becomes a tension side as shown in Figure 7e)f). When the orthogonal wall becomes compression, the reinforcing bars in the tension side yield, but the strain of bars in the compression side is small and the bars do not resist the compression force.

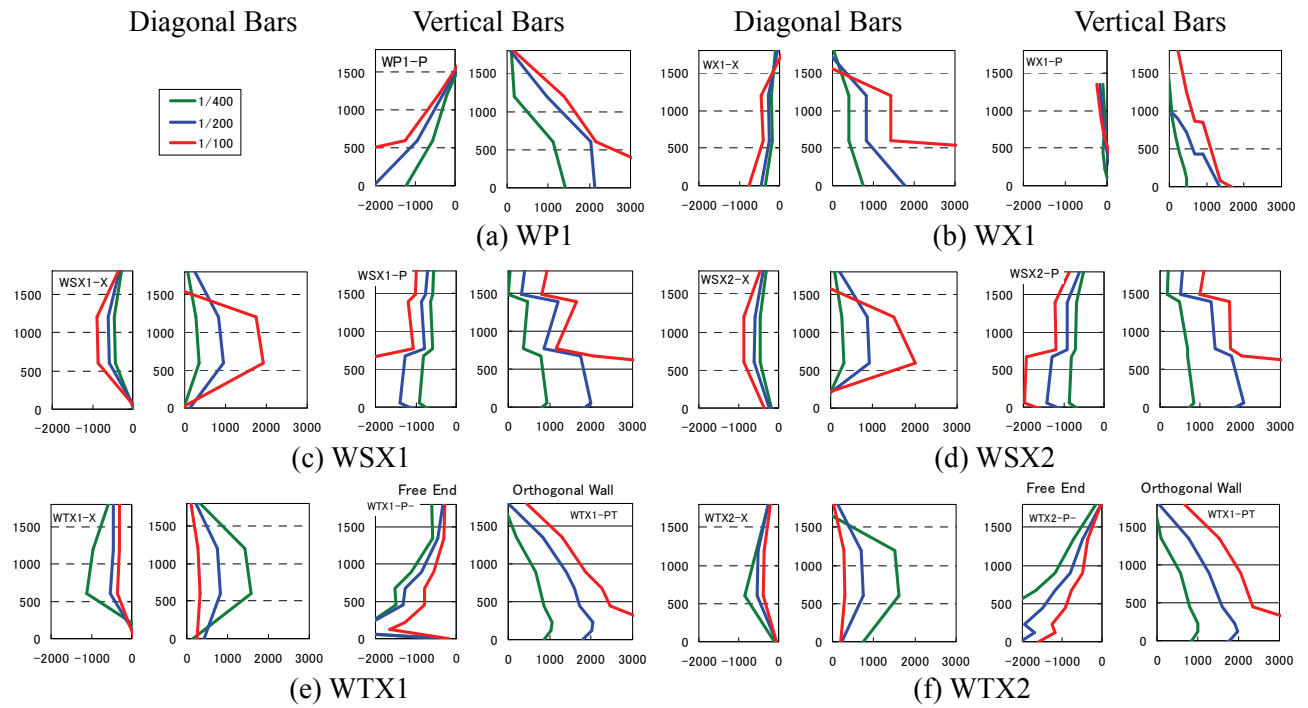


Fig.7 Strain distribution of reinforcements

4. Interpretations of test results

4.1. Load-deflection relation

The calculated value, which is the sum of the shear force at the full plastic moment of parallel reinforcements and the yield strength of the horizontal components of the diagonal reinforcements, is shown by the solid line in Figure 6. The line was modified with deflection by considering the P-Delta effect of the vertical load and the horizontal component of inclined vertical load. WP1 withstood the shear force at the full plastic moment until large deformation. The strength of WX1, WSX1 and WSX2 at large deformation was less than the calculated value. For WTX1 and WTX2, the test values were small compared with the calculated ones on the positive side where the orthogonal wall becomes a tension side. In the negative side where the orthogonal wall becomes a compression side, the tested values were quite low.

The dashed line is the calculated load-deflection relations considering the strain distribution shown in Figure 7. The compression stress of X bars is assumed to be 1/4 of the yield stress for WSX1 and 1/2 for WSX2. The test results were higher than the calculated values until large deformation. For WTX1 and WTX2, because the de-bonded X bars do not work fully, the calculation values ignored the X bars. They showed good agreement with the test results.

4.2 Bending and shear deformation

Bending deformation was calculated by integrating the curve obtained from the piecewise axial displacement difference of both wall edges. Shear deformation was calculated by subtracting the bending deformation from the total horizontal deformation. Figure 8 shows the deformation components of bending and shear deformation at the peak point of each loading cycle. The shear deformation component accounts for over 50% of the total deformation for WP1 of the common parallel reinforcing type wall. For WX1 having the de-bonded X type reinforcing bars, the bending deformation component accounts for over 80% and increases with deformation except at the final stage. This corresponds to the phenomenon that the shear crack of WX1 decreases and that the bending crack stretches to the center part. For WSX1 in which the panel wall was divided in each story, the bending deformation component accounts for over 85%, and 90% for WSX2 in which panels divided the horizontal direction into three parts. For WTX1 with the orthogonal

wall, the deformation component ratio is almost the same as the value of WX1 when the orthogonal wall is the compression side, in contrast with the tension side, and the shear deformation component becomes larger because of the large shear force caused by large bending strength. At large deformation, the compression concrete of the wall edge was crushed and slipped at the base boundary, and so the shear deformation component increased. In WTX2 which has heavy confining reinforcements in the compression area, the shear deformation component does not increase as much as WTX1, even in the case of large deformation.

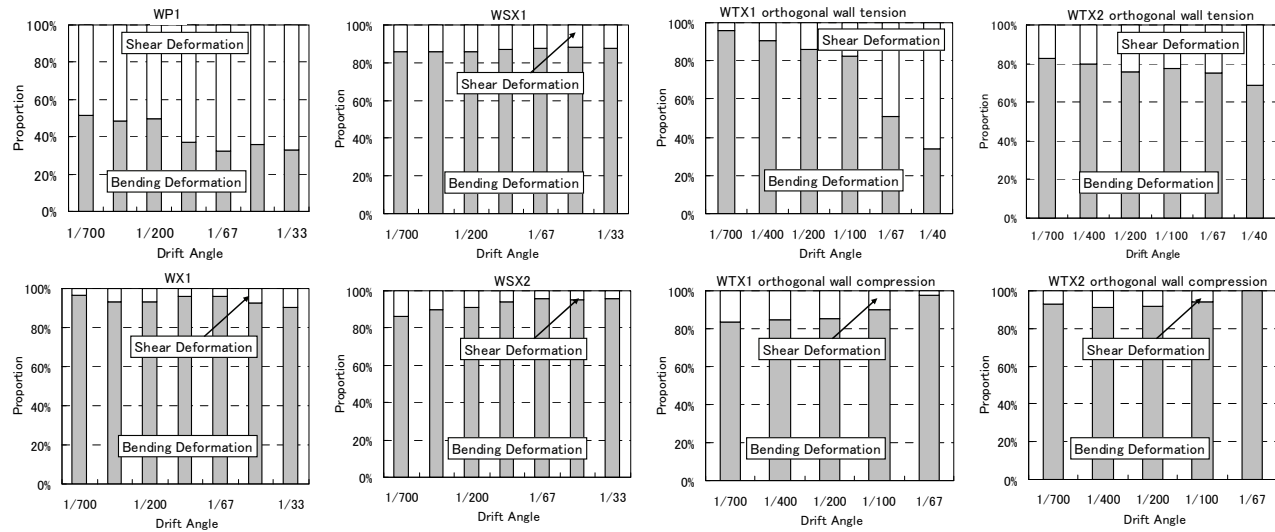


Figure 8 Bending and shear deformation

4.3 Equivalent damping factor

Figure 9 shows the equivalent damping factor of each specimen calculated from the first half cycle of the applied load – total deflection relationship shown in Figure 6.

Over $R = 1/100$, as the X bars do not yield in the compression side, the load-deflection curve shows an inverted S shape, and the equivalent damping factor of WX1 is less than that of WP1. The values of WSX1 and WSX2 are approximately equal to WX1. The damage was substantially reduced compared with WX1 but having equal energy absorbing capacity. For WTX1 and WTX2, when the orthogonal wall is in the compression side, the value is slightly larger than the value of WX1. When the orthogonal wall is in the tension side, however, the value of WTX2 with heavy confining reinforcements in the compression area is smaller than that of WTX1 because of small damage.

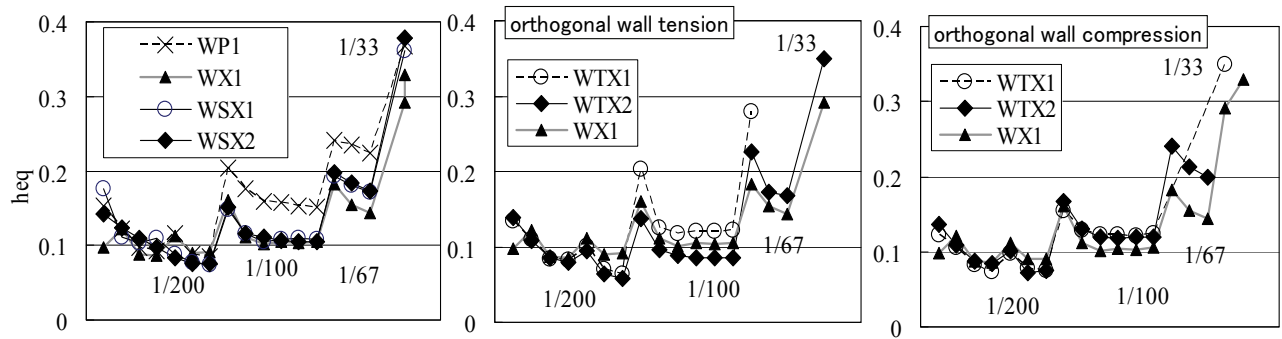


Figure 9 Equivalent damping factor

5. Conclusions

This paper examined the behavior of shear walls with de-bonded diagonal reinforcements to reduce damage during a severe earthquake for good repairability. The main findings are as follows:

1. By using de-bonded diagonal reinforcements for a core wall, the truss form is configured by the de-bonded X reinforcements and concrete struts. This reduces shear force in the panel wall and leads to good reparability with fewer cracks.
2. By forming a panel wall at each story and de-bonding the main vertical reinforcements in the panel, the bending deformation component increases with concentration in the panel boundary. As a result, shear cracks and bending cracks in the panel center do not occur, and so the wall has good repairability.
3. The horizontal strength can be calculated as the summation with shear strength of the parallel arrangement wall and the horizontal component of X bar brace yield strength with whole area of tension brace and a half area of compression brace in safe side until large deformation. The stress of concrete on the compression side becomes large because the compression X bars do not result in yielding. An adequate amount of confining reinforcement is necessary to secure deformability in the case of large deformation.
4. For the T shape core wall, the effect of the de-bonded X bars becomes less when the orthogonal wall is in tension, and it is difficult to reduce the shear cracks.

ACKNOWLEDGMENT

This study was funded by Grants-in-Aid for Scientific Research of JSPS. The opinions and findings do not necessarily represent those of the sponsor.

REFERENCES

- Shimazaki, K. (2004). De-bonded diagonally reinforced beam for good repairability, *13th World Conference on Earthquake Engineering*, **Paper 3173**.
- Satoh, H. and Shimazaki, K. (2004). Experimental research on load resistance performance of CFT column/flat plate connection, *13th World Conference on Earthquake Engineering*, **Paper 976**.
- Sittipunt, C. and wood, S. L. (2000). Development of reinforcement details to improve the cyclic response of slender structural walls, *12th World Conference on Earthquake Engineering*, **Paper 1770**.
- Yahya, C., Kurama, Y., Sause, R., Pessiki, S., and Lu, L.W. (2002). Seismic Response Evaluation of Unbonded Post-Tensioned Precast Walls, *ACI Structural Journal*, **Vol. 99, No. 5**, pp. 641-651
- FIB (2003). Seismic design of precast concrete buildings, state of art report, *fib bulletin*, **No.27**